Impact of Elevated Nitrate on Sulfate-Reducing Bacteria: A comparative Study of *Desulfovibrio vulgaris*

Qiang He[1,2], Zhili He[3,13], Dominique C. Joyner[4,13], Marcin Joachimiak[5,13], Morgan N. Price[5,13], Zamin K. Yang[6,13], Huei-Che Bill Yen[7,13], Christopher L. Hemme[3,13], Wenqiong Chen[8,13], Matthew M. Fields[9,13], David A. Stahl[12,13], Jay D. Keasling[5,11,13], Martin Keller[6,13], Adam P. Arkin[5,10,13], Terry C. Hazen[4,13], Judy D. Wall[7,13], and Jizhong Zhou[3,13*]

[1]Department of Civil and Environmental Engineering, The University of Tennessee, Knoxville, Tennessee 37966
[2]Center for Environmental Biotechnology, The University of Tennessee, Knoxville, Tennessee 37966
[3]Institute for Environmental Genomics, Department of Botany and Microbiology, University of Oklahoma, Norman, Oklahoma 73019
[4]Earth Sciences Division, Lawrence Berkeley National Laboratory, Berkeley, California 94720
[5]Physical Biosciences Division, Lawrence Berkeley National Laboratory, Berkeley, California 94720
[6]Biosciences Division, Oak Ridge National Laboratory, Oak Ridge, Tennessee 37831 [7]Departments of Biochemistry and Molecular Microbiology & Immunology, University of Missouri-Columbia, Columbia, Missouri 65211
[8]Diversa Corp, San Diego, California 92121
[9]Department of Microbiology, Montana State University, Bozeman, Montana 59171
[10]Department of Bioengineering, University of California, Berkeley, California 94720
[11]Department of Chemical Engineering, University of California, Berkeley, California 94720
[12]Department of Civil and Environmental Engineering, University of Washington, Seattle, Washington 98195
[13]Virtual Institute for Microbial Stress and Survival

*Corresponding author:

Dr. Jizhong Zhou
Institute for Environmental Genomics (IEG)
Department of Botany and Microbiology
Stephenson Research & Technology Center
University of Oklahoma
101 David L. Boren Blvd.
Norman, OK 73072
Tel: (+1) 405 325 6073
Fax: (+1) 405 325 7552
e-mail: jzhou@ou.edu

Abstract

Sulfate-reducing bacteria (SRB) have been extensively studied for their potential in heavy metal bioremediation. However, the occurrence of elevated nitrate in contaminated environments has been shown to inhibit sulfate reduction activity. While the inhibition has been suggested to result from competition with nitrate-reducing bacteria, the possibility of direct inhibition of sulfate reducers by elevated nitrate needs to be explored. Using *Desulfovibrio vulgaris* as a model sulfate-reducing bacterium, functional genomics analysis reveals that osmotic stress contributed to growth inhibition by nitrate as demonstrated by the up-regulation of the glycine/betaine transporter genes and the relief of nitrate inhibition by osmoprotectant. The observation that significant growth inhibition was affected by 70 mM $NaNO_3$ but not 70 mM NaCl suggests the presence of inhibitory mechanisms in addition to osmotic stress. The differential expression of genes characteristic of nitrite stress responses, such as the hybrid cluster protein gene, under nitrate stress condition further indicates that nitrate stress response by *D. vulgaris* was linked to components of both osmotic and nitrite stress responses. The involvement of the oxidative stress response pathway, however, might be the result of a more general stress response. Given the low similarities between the response profiles to nitrate and other stresses, less defined stress response pathways could also be important in nitrate stress, which might involve the shift in energy metabolism. The involvement of nitrite stress response upon exposure to nitrate may provide detoxification mechanisms for nitrite, which is inhibitory to SRB, produced by microbial nitrate reduction as a metabolic intermediate and enhance the survival of sulfate-reducing bacterial in environments with elevated nitrate level.

Subject Category: Integrated genomics and post-genomics approaches in microbial ecology

Keywords: *Desulfovibrio* **/** nitrate / stress response / sulfate-reducing bacteria / functional genomics / systems biology

Introduction

Exploiting microbially-mediated reduction of redox-sensitive metals has been proposed as a promising strategy to remediate metal-contaminated subsurface environments *in situ* (Valls and de Lorenzo, 2002; Wall and Krumholz, 2006). With the ability to reduce and accumulate heavy metals and radionuclides (Jones *et al.*, 1976; Lovley *et al.*, 1993; Chardin *et al.*, 2002), sulfate-reducing bacteria (SRB) have drawn particular attention for potential applications in heavy metal immobilization. It has been well documented that SRB can reductively precipitate redox metals through enzymatic pathways (Lovley and Phillips, 1992; Abdelouas *et al.*, 1998) or can simply precipitate metals as metallic sulfides. Enzymatic reduction of soluble metal oxyanions to insoluble forms has been specifically demonstrated for *Desulfovibrio* spp. (Lovley *et al.*, 1993; Lloyd *et al.*, 1999; Payne *et al.*, 2002), which are the model SRB most extensively studied for their bioremediation capacity. More importantly, SRB populations are also found to be significant members of microbial communities involved in such metal reduction and are ubiquitous even in extreme environments (Chang *et al.*, 2001; Gillan *et al.*, 2005; Bagwell *et al.*, 2006; Fields *et al.*, 2006). Therefore, stimulation of SRB activities has been considered as a useful approach for the immobilization of heavy metals and radionuclides (Landa, 2005; Lloyd and Renshaw, 2005).

To exploit SRB effectively for the remediation of heavy metal and radionuclide contaminated sites, it is important to understand the microbial responses to adverse environmental factors commonly encountered in these subsurface environments. One such factor is the high nitrate concentration of many contaminated sites at the U.S. nuclear weapon complexes managed by the Department of Energy (Riley and Zachara, 1992; NABIR, 2003). The presence of nitrate may pose a specific stress to SRB as nitrate has been observed to suppress sulfate reduction activity *in situ* (Jenneman *et al.*, 1986; Davidova *et al.*, 2001). Thus, it is important to examine the responses of sulfate-reducing microorganisms in metabolic and regulatory pathways following nitrate exposure to understand their defense mechanisms. Furthermore, since nitrate is a broadly available electron acceptor readily utilized by a large number of microorganisms in natural environments, nitrate reduction as an ecologically more competitive process could have major impacts on the survival and persistence of SRB in microbial communities as well as the functions of SRB in nitrate-impacted

environments. Therefore, insights into the mechanisms of the ecological adaptability of SRB in nitrate-impacted environments would facilitate the development of strategies to monitor and predict the performance of these microorganisms in bioremediation (Hazen and Stahl, 2006).

In this report, we used *Desulfovibrio vulgaris* Hildenborough as a model organism to investigate the inhibition of sulfate reduction by nitrate as compared to other related stress conditions. Our results from physiological analyses indicate the presence of inhibitory mechanisms in addition to the expected osmotic stress responses. Subsequent functional studies revealed that nitrate stress response by *D. vulgaris* was linked to components of both osmotic and nitrite stress responses.

Materials and methods

High throughput monitoring of cell growth with various stressor concentrations

The growth response of *D. vulgaris* cells to various concentrations of sodium nitrate ($NaNO_3$) or sodium chloride (NaCl) were monitored using the Phenotype MicroArray™ platform (Biolog Inc., Hayward, CA). Culture handling and instrument operation were carried out following a previously described procedure (Borglin *et al.*, 2009). The OmniLog® instrument was calibrated against *D. vulgaris* cell densities as measured by a spectrophotometer at OD_{600} and direct cell counts. All were comparable at 95% confidence interval (CI) for the exponential growth phase. Specifically, OL (Omnilog) readings were converted to cell density (cells/ml) with the following experimentally determined linear expression (r^2=0.933, n=37): cell density = $2.34\times10^7\cdot$OL+34.3.

Impacts of osmoprotectant on growth responses to nitrate stress

Glycine betaine was selected as the osmoprotectant to test the presence of potential osmotic stress responses when *D. vulgaris* was exposed to high nitrate levels since this osmolyte had been shown to protect *D. vulgaris* from salt stress (Mukhopadhyay *et al.*, 2006). Initially, glycine betaine was added into the Yen45 defined medium (Bender *et al.*, 2007) to a final concentration of 2 mM, together with additional $NaNO_3$ at 100 or 200 mM. This medium has fewer precipitates that interfere with optical density determinations than does LS4D. Controls without glycine betaine and those without either

glycine betaine or nitrate were also compared. Following a 2% (v/v) inoculation with a late-log phase culture (OD_{600}~0.8-0.9) growth was monitored by optical density measurements at 600 nm.

Biomass production for microarray and proteomics analysis

Cultures for biomass production were initiated with 10 % (v/v) inocula from stocks of *D. vulgaris* frozen at -80° C (fully grown cells in LS4D with 10% (v/v) glycerol) into LS4D medium as previously described (Mukhopadhyay *et al.*, 2006). All production cultures were grown in triplicate (three control cultures and three stressed cultures). When the production cultures reached an OD_{600} of 0.3, 50 ml were taken from each replicate culture as the T0 samples. Once the T0 samples were taken, degassed $NaNO_3$ solution was immediately added to the three treatment cultures to a final concentration of 105 mM (6500 ppm nitrate, which was shown to inhibit the growth rate of the log-phase cultures by approximately 50%), and an equivalent volume of sterile, distilled, degassed water was added to each control culture. Culture samples of 50 ml were collected from each culture at 30, 60, 120, and 240 min post-addition while cells were still in exponential growth phase. To minimize mRNA or protein changes during sample collection and processing, cell samples were rapidly chilled and pelleted using a previously described method (Mukhopadhyay *et al.*, 2006). The final pellet was flash-frozen in liquid nitrogen and stored at –80°C for microarray analysis.

The same procedure was followed to collect biomass for proteomics analysis with the exception that sampling from the production cultures was conducted at only two time points. Briefly, when the production cultures reached an OD_{600} of ca. 0.3, 100 ml of sample were taken from each triplicate culture as the T0 samples. Following nitrate (105 mM) addition, 100 ml each from the 3 control cultures and 100 ml each from the 3 stressed cultures were collected at 240 min post-exposure as the T1 samples. Culture samples from the triplicate treatment or control cultures at each time point were subsequently pooled to provide adequate biomass for protein extraction. Cell mass from the four pooled culture samples, T1 and T0 for the treatment or control, were harvested using the same procedure as described above for microarray analysis. The final pellet was flash-frozen in liquid nitrogen and stored at –80°C until proteomics analysis.

Microarray transcriptomic analysis

A previously described whole-genome oligonucleotide DNA microarray (He *et al.*, 2006), covering more than 98.6% of the annotated protein-coding sequences of the *D. vulgaris* genome, was used for global transcriptional analysis of nitrate stress response. The accuracy of the microarrays in global transcriptional profiling has been extensively tested and validated in previous studies on stress response pathways in *D. vulgaris* (Clark *et al.*, 2006; He *et al.*, 2006). All microarray procedures including the extraction and labeling of nucleic acids, microarray hybridization and washing, and data analysis were performed using previously published protocols (He *et al.*, 2006). Total RNA extraction, purification, and labeling were performed independently on each cell sample using previously described protocols (He *et al.*, 2006; Butler *et al.*, 2007). Each replicate sample consisted of cells from 300-ml cultures. Labeling of cDNA targets from purified total RNA was carried out using the reverse transcriptase reaction with random hexamer priming, and the fluorophore Cy5-dUTP (Amersham Biosciences, Piscataway, NJ). Genomic DNA was extracted from *D. vulgaris* cultures at stationary phase and labeled with the fluorophore Cy3-dUTP (Amersham Biosciences, Piscataway, NJ). To hybridize a single glass slide, the Cy5-dUTP-labeled cDNA targets obtained from stressed or non-stressed control cultures were mixed with the Cy3-dUTP-labeled genomic DNA. After washing and drying, the microarray slides were scanned using the ScanArray Express microarray analysis system (Perkin Elmer, Fremont, CA). The fluorescent intensity of both Cy5 and Cy3 fluorophores was analyzed with ImaGene software version 6.0 (Biodiscovery, Marina Del Rey, CA). Log ratios of differential gene expression between treatment and control cultures were determined using previously described data processing and analysis methods and statistical significance was assessed by standard Z-scores (Chhabra *et al.*, 2006). Pairwise correlation coefficients between any two transcriptional profiles were computed with the centered Pearson correlation using the entire transcriptional expression profiles obtained by the *D. vulgaris* microarray. Color heat map representations comparing gene expression under various growth conditions were generated using the software JColorGrid (Joachimiak *et al.*, 2006). The microarray results were deposited at the GEO database with the accession number GSE20079.

Three-dimensional nano LC-MS/MS proteomics analysis of nitrate-stressed biomass

Total protein extracted and treated from the control and stressed samples were used for fractionation by three-dimensional liquid chromatography (LC), followed by tandem mass spectrometry (MS/MS) analysis to determine the protein identities, as described previously (Wei *et al.*, 2005). The relative abundance of proteins in each sample was estimated based on the hypothesis that the more abundant a peptide ion is in a mixture, the more likely the peptide ion is sampled during the course of an MS/MS experiment (Wolters *et al.*, 2001; Liu *et al.*, 2004). Accordingly, the total numbers of qualified spectral counts represented the relative abundance of each protein under a specific condition. To identify proteins for which there were significant changes under certain conditions, the statistical "local-pooled-error" test (Jain *et al.*, 2003) was used. Only protein changers with a *p*-value of less than 0.05 were considered to be significant.

Results

Growth inhibition of D. vulgaris by nitrate

The inhibitory effect of nitrate was evaluated by monitoring the growth of *D. vulgaris* in the presence of various concentrations of sodium nitrate. While a slow-growth phase (with no detectable growth) of approximately 20 hours was observed in control cultures without nitrate addition, an extended phase of slow growth followed by normal growth was observed with increasing concentrations of nitrate in the culture medium, indicative of a moderate inhibitory effect (Figure 1A). A more severe inhibition pattern, characterized by a sharp decrease in growth rate accompanied by an increasingly longer slow-growth phase, was apparent when the nitrate concentration reached 70 mM, as indicated by the reduced slope of the growth curve (Figure 1A).

Since sodium nitrate is an ionic solute, high concentrations of nitrate are expected to result in osmotic stress as a non-specific inhibitory mechanism. To identify any inhibitory effects specific to nitrate, a comparison was made between the growth responses of *D. vulgaris* to sodium nitrate versus sodium chloride, known to cause osmotic stress. In sharp contrast to the 70 mM sodium nitrate addition needed for growth inhibition, a significant decrease in the growth rate of *D. vulgaris* was

observed only when 200 mM sodium chloride was added into the LS4D medium (Figure 1B). These results suggest that sodium nitrate inhibition resulted from at least some interactions specific to nitrate and not simply from a salt-induced osmotic effect.

Global transcriptomic analysis of nitrate stress

To understand the mechanisms of nitrate inhibition and the potential response pathways used by *D. vulgaris* cells to alleviate nitrate stress, microarray experiments were carried out to compare global gene expression profiles between nitrate-stressed *D. vulgaris* cultures and control cultures without nitrate exposure. *D. vulgaris* cells were challenged by a nitrate level of 105 mM, which was effective in inhibiting, but not eliminating, cell growth in log-phase cultures.

Changes in the gene expression profile were observed at 30 min following nitrate exposure and peaked at 120 min, with 298 genes being differentially expressed, either up or down, greater than two fold (Figure S1). A similar number of genes (288) remained differentially regulated at 240 min. It is noted that the number of genes with reduced expression level considerably exceeded the number of genes with increased expression at 30, 60, and 120 min, consistent with the inhibitory effect of nitrate observed in the growth study (Figure 1). As the number of down-regulated genes peaked at 120 min, the number of up-regulated genes, however, continued to rise throughout the duration of the experiment, indicative of an active response to nitrate treatment following the initial inhibition.

Effects of osmoprotectant on growth inhibition by nitrate

Given the presence of osmotic stress at high nitrate concentrations, indications of osmotic stress response following nitrate exposure were examined. Indeed, transcriptional profiling showed an increase in the gene expression of the periplasmic-binding protein of the glycine/betaine/proline ABC transporter (DVU2297; $\log_2 R = 1.6$ at 240 min), although not the putative permease or ATP binding protein. Since glycine betaine is a known osmoprotectant (Cayley and Record, 2003) and has been shown to relieve osmotic stress in *D. vulgaris* (Mukhopadhyay *et al.*, 2006), the up-regulation of this gene supports the expected overlap between osmotic stress and nitrate stress. To further confirm that nitrate inhibition is associated with osmotic stress, growth was monitored following the addition of

glycine betaine as an osmoprotectant into *D. vulgaris* cultures in nitrate-supplemented defined medium (Figure 2).

Similar to stress-inducing concentrations of NaCl, elevated $NaNO_3$ concentrations resulted in a prolonged lag phase and significantly reduced final cell density. The addition of glycine betaine led to the complete recovery of the final cell density in *D. vulgaris* cultures exposed to 100 mM $NaNO_3$; but provided only a 16% reduction of the lag phase (Figure 2A), which is in contrast to the near complete reversal of growth inhibition by glycine betaine in NaCl stress (Mukhopadhyay *et al.*, 2006). The inability of glycine betaine to relieve nitrate stress entirely indicates that osmotic stress does not account for all the inhibition of cellular activities by nitrate stress.

In contrast, growth inhibition by 200 mM $NaNO_3$ was more significantly relieved by the inclusion of glycine betaine in the medium, with the lag phase shortened from approximately 300 h to 100 h (Figure 2B). This observation was likely the result of the increasing importance of osmotic stress with higher levels of nitrate. Nonetheless, only partial relief of nitrate stress was provided by the addition of osmoprotectant, further suggesting the presence of additional sources of growth inhibition that were specific to nitrate stress, but not osmotic stress.

Genes involved in methyl/SAM metabolism

In nitrate-stressed *D. vulgaris,* a group of genes involved in the methyl metabolism were among those with the greatest increases in expression (Table S1), including *metF* (DVU0997), *metE* (DVU3371), and *ahcY* (DVU0607). All these genes have functions in the metabolism of methionine and regeneration of *S*-adenosylmethionine (SAM), a major methyl-donor in various cellular processes (Wang and Frey, 2007). A careful examination of the genes up-regulated under nitrate stress further revealed the increased expression of the gene encoding another key enzyme in SAM biosynthesis, *S*-adenosylmethionine synthetase MetK (DVU2449; $\log_2 R = 1.7$). From the co-expression patterns of all these genes (Figure S2), scattered across the genome, we infer the presence of a regulatory mechanism that might be involved in the increased turnover of SAM.

Interestingly, the enzyme activating the pyruvate formate-lyase (DVU2825), which was also among the most up-regulated genes under nitrate stress (Table S1), has been shown to require the

methyl-donor SAM in other bacteria (Chase and Rabinowitz, 1968; Knappe and Schmitt, 1976), providing a potential link between energy metabolism and methyl/SAM metabolism (Figure S2).

Genes involved in energy metabolism

Nitrate does not support growth of *D. vulgaris* as an electron acceptor or nitrogen source (Haveman *et al.*, 2004; Haveman *et al.*, 2005). However, in many other anaerobes nitrate metabolism is directly linked to energy metabolism via multiple redox reactions (Moura *et al.*, 1997). Thus, the involvement of genes in energy metabolism was investigated when elevated nitrate constituted a stress condition. Transcriptional analysis indicated that a small number of genes with functions in energy metabolism were among those highly up-regulated under nitrate stress, such as the genes related to the catabolism of pyruvate as a key metabolic intermediate: a pyruvate formate-lyase (DVU2824) and its activating enzyme (DVU2825) (Table S1). These two genes form an operon with two other genes encoding a TRAP dicarboxylate transporter (DVU2822-2825). In addition, a formate dehydrogenase gene cluster (DVU0586-0588) had increased expression under nitrate stress (data not shown). The composite of these differentially expressed genes appears to be consistent with an increased flow of reducing equivalent cycling through formate as a metabolic intermediate, as suggested under certain growth conditions (He *et al.*, 2006; Pereira *et al.*, 2008).

The gene encoding the hybrid cluster protein (DVU2543), which was suggested to be involved in the response to reactive nitrogen species generated in nitrate metabolism in other microorganisms (van den Berg *et al.*, 2000; Wolfe *et al.*, 2002), was also up-regulated ($\log_2$R = 1.8). It is noted that this gene was among the most highly up-regulated ($\log_2$R = 6.4) under nitrite stress (Haveman *et al.*, 2004; He *et al.*, 2006). The iron-sulfur cluster-binding protein, predicted to be encoded promoter distal in the same operon (DVU2544), was also increased in expression ($\log_2$R = 1.9), representing a shared response to nitrate and nitrite stress (Table 1). Nonetheless, the differential expression of the hybrid cluster protein operon was much weaker in response to nitrate than that to nitrite. No significant changes in gene expression were observed in other known genes participating in nitrogen metabolism.

Another highly up-regulated gene with annotated functions in energy metabolism encodes a putative rubrerythrin (DVU2318) (Table S1), which is predicted to be under the regulation of the Peroxide-Responsive Regulator (PerR) (Rodionov *et al.*, 2004). A survey of the gene expression profile indicated that all genes in the predicted PerR regulon had increased expression to various extents under nitrate stress (Table 2). However, comparison of gene expression profiles found that the PerR regulon was consistently up-regulated throughout different stress conditions (Chhabra *et al.*, 2006; He *et al.*, 2006; Mukhopadhyay *et al.*, 2006; Mukhopadhyay *et al.*, 2007), indicating that the increased expression of the PerR regulon was likely a part of the general stress response.

Proteomics analysis of nitrate stress response

LC-MS/MS proteomics analysis of the stress response to nitrate in the wild-type strain was performed to complement transcriptional analysis. Ribosomal proteins were among the most down-regulated, consistent with transcriptional analysis and growth inhibition observed with exposure to elevated nitrate (Table 3). Proteomics results also confirmed the up-regulation of the glycine/betaine/proline ABC transporter (DVU2297) and MetE (DVU3371), which is a key enzyme in the methyl/SAM metabolic pathway (Figure S2). A *phi* coefficient of correlation of 0.6 was achieved for genes/proteins with significant changes in both transcriptional and proteomics analyses, indicative of the good agreement on the direction of regulation at both the messenger RNA and protein levels. This is also largely consistent with prior comparisons between transcriptional and proteomics profiles in *D. vulgaris* (Chhabra *et al.*, 2006; Mukhopadhyay *et al.*, 2006), confirming the validity of the microarray technique and subsequent transcriptional analysis for making regulatory event inferences in *D. vulgaris*.

Comparison of nitrate stress response with other stress conditions

The above analyses show that nitrate stress shared with two related stresses, NaCl stress and nitrite stress, similar patterns of gene expression in a number of genes, including the glycine/betaine/proline ABC transporter (DVU2297) and hybrid cluster protein (DVU2543) genes. To further determine potential correlations in gene expression between nitrate, nitrite, and NaCl stress responses in *D.*

vulgaris, all genes with significant changes in expression were identified at 30 min following stress exposure, which corresponds to the earliest post-stress time point and likely represents the most direct stress responses in the early phase of the stress experiments. Genes with changes in expression at later post-stress time points, however, might not necessarily be representative of nitrate-specific responses. Instead, these genes could be involved in general stress response subsequent to the nitrate-specific primary responses, such as the genes characteristic of the general oxidative stress responses in the PerR regulon discussed above, which were significantly up-regulated at later time points during the experimental period (Table 2).

It is revealed that there were variable numbers of differentially expressed genes in response to each stress, from 40 in nitrate stress and 60 in salt stress (Mukhopadhyay *et al.*, 2006), to 261 in nitrite stress (He *et al.*, 2006) (Figure S3). The numbers of differentially expressed genes in common between these experiments were very few, with ten between nitrite and NaCl, six between nitrate and nitrite, one between nitrate and NaCl, and none among all three stress responses. Thus, when considering common genes with significant change in expression at the time point when the stress response was most expected (30 min), it is evident there was little similarity between these stress responses.

To further examine the presence of stress response pathways common between nitrate stress and various other stress conditions, analyses of gene expression overlap proportions and correlations were performed across all pairs of time points in 8 stress responses including nitrate (this study), nitrite (He *et al.*, 2006), NaCl and KCl (Mukhopadhyay *et al.*, 2006), heat shock (Chhabra *et al.*, 2006), low oxygen (1000 ppm) (Mukhopadhyay *et al.*, 2007), high oxygen (air) (Mukhopadhyay *et al.*, 2007), and alkaline stress (Stolyar *et al.*, 2007). The highest values for gene overlap proportions (Figure 3) and gene expression correlations (Figure S4) were observed between time points of the same stress response, as expected. Considering comparisons across different stress responses at 30 min post-stress, the two salt stresses NaCl and KCl showed the largest gene expression overlap proportions among all experimental pairs (excluding comparisons of time points from the same experiment) (Figure 3) and the highest correlation of 0.71 at 30 min (Figure S4). The heat shock and high oxygen (air) stress exhibited the second largest overlap proportion and a correlation of 0.51 at 30 min (Figure

3 & S4), indicative of the similarities in stress response. It is evident that stress pairs showing the most gene expression overlap and highest gene expression correlations did so at all time points following the stress treatment. In contrast, the comparisons between nitrate, nitrite, and NaCl showed minimal gene overlap proportions and gene expression correlations (Figure 3 & S4). For example, the gene expression correlation at 30 min for nitrate and nitrite was 0.08, for nitrate and NaCl 0.11, and for nitrite and NaCl 0.19. Slightly better gene expression overlap proportions were observed between the last nitrate stress time point at 240 min and selected nitrite stress time points. Similarly, the last nitrate stress time point had low overlap of gene expression with several NaCl time points. Since the last time point in the nitrate stress may not represent a primary response to this stress but secondary effects, these low similarity measures do not support similarity between the nitrate, nitrite, and NaCl responses.

Discussion

Nitrate is a common co-contaminant in subsurface environments impacted by radionuclides and heavy metals (Brooks, 2001). Nitrate inhibition of metal-reducing microbial populations, such as the sulfate-reducing bacteria, hinders bioremediation efforts exploiting these microbial biocatalysts (Abdelouas *et al.*, 1998; Finneran *et al.*, 2002; Istok *et al.*, 2004; Nyman *et al.*, 2006). However, the persistence of sulfate-reducing bacteria at contaminated sites with high nitrate levels suggested the presence of potential resistance mechanisms (Gu *et al.*, 2005; Bagwell *et al.*, 2006; Fields *et al.*, 2006), which were explored in this study using physiological and genomics approaches.

Growth inhibition by nitrate in the form of osmotic stress was demonstrated by the up-regulation of the glycine/betaine transporter genes and the relief of nitrate inhibition by osmoprotectant (Figure 2). However, osmotic stress response is not likely the only pathway contributing to the inhibitory effect of nitrate, given the minimal similarity in the transcriptional profiles between nitrate stress and NaCl stress (Figure 3 & S4). Indeed, the finding that *D. vulgaris* cells were significantly more sensitive to $NaNO_3$ than NaCl (Figure 1) indicates the involvement of inhibitory mechanisms in addition to the osmotic stress resulting from elevated nitrate concentrations. Presumably, the more

severe growth inhibition under nitrate stress (Figure 1A) could be attributed to the presence of the nitrate ions, as compared to chloride ions.

Differing from Cl^-, in some bacteria, the nitrate ion is redox active and can serve as a terminal electron acceptor in energy metabolism or as a source of nitrogen for biosynthesis, both requiring the reduction of nitrate coupled with electron transfer. However, nitrate-dependent growth of *D. vulgaris* has not been observed, which is consistent with the absence of nitrate reductase genes in the sequenced genome of *D. vulgaris* (Moura *et al.*, 1997; Haveman *et al.*, 2004; Heidelberg *et al.*, 2004). Thus, it is unlikely that copious amounts of nitrogenous intermediates would be generated as toxic intermediates from nitrate reduction in *D. vulgaris*. It is suggested, however, that small amounts of nitrite, and subsequently other reactive nitrogen species, could be produced from non-specific reduction of nitrate by low potential reductases in *D. vulgaris* cells, such as the multiheme *c*-type cytochromes (Wall *et al.*, 2007). Due to the specificity of nitrite toxicity to sulfate reduction (Greene *et al.*, 2003; Haveman *et al.*, 2004), nitrite derived from nitrate could represent a major stress condition for *D. vulgaris*. It appears that the significant up-regulation of the hybrid cluster protein genes (DVU2543-2544) upon nitrate exposure (Table 1), which resembled a similar response pattern specific to nitrite stress (Greene *et al.*, 2003; Haveman *et al.*, 2004; He *et al.*, 2006), would support the suggestion that nitrite stress is a result of nitrate exposure.

The initiation of nitrite stress responses upon exposure to nitrate in *D. vulgaris* could be of particular ecological significance in the persistence of SRB in environments with elevated levels of nitrate, which has been shown to effectively inhibit SRB populations in the environment (Jenneman *et al.*, 1986; Davidova *et al.*, 2001). More importantly, the nitrate inhibition of SRB is shown to be caused by nitrite, a key intermediate during microbial nitrate reduction (Greene *et al.*, 2003; Voordouw *et al.*, 2009). Thus, given the known toxicity of nitrite to SRB (Haveman *et al.*, 2004; He *et al.*, 2006), a potential impact of nitrate stress on SRB in natural environment could be the subsequent occurrence of nitrite stress with the onset of microbial nitrate reduction. Even though nitrate can not serve as an electron acceptor for *D. vulgaris*, nitrate is a common electron acceptor readily utilized by many other microorganisms. As a result, the presence of nitrate in the environment would rapidly result in the production of nitrite via microbial nitrate reduction. The initiation of stress

responses for nitrite detoxification upon nitrate exposure, therefore, would prepare SRB population for the imminent inhibitory effects of nitrite produced from nitrate reduction and provide a physiological advantage to the survival of SRB in the environment.

Aside from components of salt stress and nitrite stress, involvement of oxidative stress response was also implicated during nitrate stress in *D. vulgaris*, with the up-regulation of the genes in the PerR regulon (Table 2), which is known to be responsive to oxidative stress (Rodionov *et al.*, 2004). However, examination of the responses of *D. vulgaris* to other stress conditions reveals that the up-regulation of the Per-R regulon under not only oxygen stress (Mukhopadhyay *et al.*, 2007), but also nitrite (He *et al.*, 2006), salt (Mukhopadhyay *et al.*, 2006), and heat (Chhabra *et al.*, 2006) stress, suggesting the response of the PerR regulon may not be specifically linked to nitrate. The same non-specific response could also be suggested for several other genes responsive to nitrate stress. For example, the gene for the phage shock protein A (DVU2988) was up-regulated in nitrate stress (Table S1). However, this gene was also up-regulated under conditions of salt (Mukhopadhyay *et al.*, 2006), heat (Chhabra *et al.*, 2006), and oxygen (Mukhopadhyay *et al.*, 2007) stress, suggesting that this response was not directly related to nitrate stress, rather a form of general stress response.

In contrast, energetic consequences of nitrate stress could be considered as potential mechanisms contributing to the inhibition of *D. vulgaris* by nitrate. Indeed, our results indicate that a number of genes with functions in energy metabolism were among those highly up-regulated under nitrate stress, such as an operon consisting of genes related to the catabolism of pyruvate as a key metabolic intermediate, a pyruvate formate-lyase (DVU2824) and its activating enzyme (DVU2825), as well as another operon encoding a formate dehydrogenase (DVU0586-0588) (Table 1). These regulatory events implicate a shift in energy metabolism to the increased flow of reducing equivalents through formate as a metabolic intermediate during nitrate stress. Notably, the activation of the pyruvate formate-lyase (DVU2824), a key enzyme in the generation of formate from the central metabolite pyruvate, has been shown to require the methyl-donor SAM in other bacteria (Chase and Rabinowitz, 1968; Knappe and Schmitt, 1976). The increased flow of reducing equivalent during nitrate exposure could potentially be used by *D. vulgaris* as a mechanism to meet the demand for an increased electron flow by redox processes, such as the detoxification of nitrite (He *et al.*, 2006) generated from the

reduction of nitrate by other microbial populations, thus providing a physiological advantage to the survival of these microorganisms in natural environments with high nitrate levels. Interestingly, genes involved in methyl/SAM metabolism were among the most responsive to nitrate stress in *D. vulgaris* (Table S1), thus linking the methyl/SAM metabolic pathway to the shift in energy metabolism (Figure S2). However, a definitive relationship between the shift in energy metabolism and nitrate inhibition could not be established, given the limited scope of this study. Future work should be focused on the elucidation of the roles of the energy metabolism in nitrate stress.

Therefore, the response to nitrate stress by *D. vulgaris* was shown to be linked to components of both osmotic and nitrite stress responses (Figure 4), which is illustrated by the up-regulation of the glycine/betaine transporter genes known to relieve salt stress (Mukhopadhyay *et al.*, 2006) and the hybrid cluster protein gene identified specifically in nitrite stress (He *et al.*, 2006). Nitrate stress also impacted energy metabolism by increased expression of the SAM/methyl cycle, along with the up-regulation of the pyruvate formate-lyase, resulting in a shift to the increased flow of reducing equivalents through formate as a metabolic intermediate. The increased flux of formate is likely processed by the periplasmic formate dehydrogenase, which was expressed at a higher level during nitrate stress. The involvement of the oxidative stress response pathway, however, might be the result of a more general stress response. Given the low similarities between the response profiles to nitrate and other stresses, less defined stress response pathways could also be important in nitrate stress, which might involve the shift in energy metabolism.

Acknowledgement

This work was part of the Environmental Stress Pathway Project (ESPP) of the Virtual Institute for Microbial Stress and Survival (http://vimss.lbl.gov) supported by the U. S. Department of Energy, Office of Science, Office of Biological and Environmental Research, Genomics: GTL Program, through contract DE-AC02-05CH11231 with Lawrence Berkeley National Laboratory.

References

Abdelouas A, Lu YM, Lutze W, Nuttall HE. (1998). Reduction of U(VI) by indigenous bacteria in contaminated ground water. *J Contam Hydrol* **35**: 217-233.

Bagwell CE, Liu X, Wu L, Zhou J. (2006). Effects of legacy nuclear waste on the compositional diversity and distributions of sulfate-reducing bacteria in a terrestrial subsurface aquifer. *FEMS Microbiol Ecol* **55**: 424-431.

Bender KS, Yen H-CB, Hemme CL, Yang Z, He Z, He Q *et al.* (2007). Analysis of a ferric uptake regulator (Fur) mutant of *Desulfovibrio vulgaris* Hildenborough. *Appl Environ Microbiol* **73**: 5389-5400.

Borglin S, Joyner D, Jacobsen J, Mukhopadhyay A, Hazen TC. (2009). Overcoming the anaerobic hurdle in phenotypic microarrays: Generation and visualization of growth curve data for *Desulfovibrio vulgaris* Hildenborough. *J. Microbiol. Methods* **76**: 159-168.

Brooks SC. (2001). Waste characteristics of the former S-3 ponds and outline of uranium chemistry relevant to NABIR Field Research Center studies ORNL/TM-2001/27. NABIR Field Research Center: Oak Ridge, TN.

Butler JE, He Q, Nevin KP, He Z, Zhou J, Lovley DR. (2007). Genomic and microarray analysis of aromatics degradation in *Geobacter metallireducens* and comparison to a *Geobacter* isolate from a contaminated field site. *BMC Genomics* **8**: 180.

Cayley S, Record MT, Jr. (2003). Roles of cytoplasmic osmolytes, water, and crowding in the response of *Escherichia coli* to osmotic stress: biophysical basis of osmoprotection by glycine betaine. *Biochemistry* **42**: 12596-12609.

Chang Y-J, Peacock AD, Long PE, Stephen JR, McKinley JP, MacNaughton SJ *et al.* (2001). Diversity and characterization of sulfate-reducing bacteria in groundwater at a uranium mill tailings site. *Appl Environ Microbiol* **67**: 3149-3160.

Chardin B, Dolla A, Chaspoul F, Fardeau ML, Gallice P, Bruschi M. (2002). Bioremediation of chromate: thermodynamic analysis of the effects of Cr(VI) on sulfate-reducing bacteria. *Appl Environ Microbiol* **60**: 352-360.

Chase T, Rabinowitz JC. (1968). Role of pyruvate and *S*-adenosylmethionine in activating the pyruvate formate-lyase of *Escherichia coli*. *J Bacteriol* **96**: 1065-1078.

Chhabra SR, He Q, Huang KH, Gaucher SP, Alm EJ, He Z *et al.* (2006). Global analysis of heat shock response in *Desulfovibrio vulgaris* Hildenborough. *J Bacteriol* **188**: 1817-1828.

Clark ME, He Q, He Z, Huang KH, Alm EJ, Wan X-F *et al.* (2006). Temporal transcriptomic analysis as *Desulfovibrio vulgaris* Hildenborough transitions into stationary phase during electron donor depletion. *Appl Environ Microbiol* **72**: 5578-5588.

Davidova I, Hicks MS, Fedorak PM, Suflita JM. (2001). The influence of nitrate on microbial processes in oil industry production waters. *J Ind Microbiol Biotechnol* **27**: 80-86.

Fields MW, Bagwell CE, Carroll SL, Yan T, Liu X, Watson DB *et al.* (2006). Phylogenetic and functional biomakers as indicators of bacterial community responses to mixed-waste contamination. *Environ Sci Technol* **40**: 2601-2607.

Finneran KT, Housewright ME, Lovley DR. (2002). Multiple influences of nitrate on uranium solubility during bioremediation of uranium-contaminated subsurface sediments. *Environ Microbiol* **4**: 510-516.

Gillan DC, Danis B, Pernet P, Joly G, Dubois P. (2005). Structure of sediment-associated microbial communities along a heavy metal contaminated gradient in the marine environment. *Appl Environ Microbiol* **71**: 679-690.

Greene EA, Hubert C, Nemati M, Jenneman GE, Voordouw G. (2003). Nitrite reductase activity of sulfate-reducing bacteria prevents their inhibition by nitrate-reducing, sulfide-oxidizing bacteria. *Environ Microbiol* **5**: 607-617.

Gu B, Wu W-M, Ginder-Vogel MA, Yan H, Fields MW, Zhou J *et al.* (2005). Bioreduction of uranium in a contaminated soil column. *Environ Sci Technol* **39**: 4841-4847.

Haveman SA, Greene EA, Stilwell CP, Voordouw JK, Voordouw G. (2004). Physiological and gene expression analysis of inhibition of *Desulfovibrio vulgaris* Hildenborough by nitrite. *J Bacteriol* **186**: 7944-7950.

Haveman SA, Greene EA, Voordouw G. (2005). Gene expression analysis of the mechanism of inhibition of *Desulfovibrio vulgaris* Hildenborough by nitrate-reducing, sulfide-oxidizing bacteria. *Environ Microbiol* **7**: 1461-1465.

Hazen TC, Stahl DA. (2006). Using the stress response to monitor process control: pathways to more effective bioremediation. *Curr Opin Biotechnol* **17**: 285-290.

He Q, Huang KH, He Z, Alm EJ, Fields MW, Hazen TC *et al.* (2006). Energetic consequences of nitrite stress in *Desulfovibrio vulgaris* Hildenborough, inferred from global transcriptional analysis. *Appl Environ Microbiol* **72**: 4370-4381.

Heidelberg JF, Seshadri R, Haveman SA, Hemme CL, Paulsen IT, Kolonay JF *et al.* (2004). The genome sequence of the anaerobic, sulfate-reducing bacterium *Desulfovibrio vulgaris* Hildenborough. *Nature Biotechnol* **22**: 554-559.

Istok JD, Senko JM, Krumholz LR, Watson D, Bogle MA, Peacock A *et al.* (2004). In situ bioreduction of technetium and uranium in a nitrate-contaminated aquifer. *Environ Sci Technol* **38**: 468-475.

Jain N, Thatte J, Braciale T, Ley K, O'Connell M, Lee JK. (2003). Local-pooled-error test for identifying differentially expressed genes with a small number of replicated microarrays. *Bioinformatics* **19**: 1945-1951.

Jenneman GE, McInerney MJ, Knapp RM. (1986). Effect of nitrate on biogenic sulfide production. *Appl Environ Microbiol* **51**: 1205-1211.

Joachimiak MP, Weissman JL, May BCH. (2006). JColorGrid: software for the visualization of biological measurements. *BMC Bioinformatics* **7**: 225.

Jones HE, Trudinger PA, Chambers LA, Pyliotis NA. (1976). Metal accumulation by bacteria with particular reference to dissimilatory sulfate-reducing bacteria. *Z Allg Mikrobiol* **16**: 425-435.

Knappe J, Schmitt T. (1976). A novel reaction of *S*-adenosyl-L-methionine correlated with the activation of pyruvate formate-lyase. *Biochem Biophys Res Commun* **71**: 1110-1117.

Landa ER. (2005). Microbial biogeochemistry of uranium mill tailings. *Adv Appl Microbiol* **57**: 113-130.

Liu H, Sadygov RG, Yates JR, III. (2004). A model for random sampling and estimation of relative protein abundance in shotgun proteomics. *Anal Chem* **76**: 4193-4201.

Lloyd JR, Renshaw JC. (2005). Bioremediation of radioactive waste: radionuclide–microbe interactions in laboratory and field-scale studies. *Curr Opin Biotechnol* **16**: 254-260.

Lloyd JR, Ridley J, Khizniak T, Lyalikova NN, Macaskie LE. (1999). Reduction of technetium by *Desulfovibrio desulfuricans*: biocatalyst characterization and use in a flowthrough bioreactor. *Appl Environ Microbiol* **65**: 2691-2696.

Lovley DR, Phillips EJP. (1992). Reduction of uranium by *Desulfovibrio desulfuricans*. *Appl Environ Microbiol* **58**: 850-856.

Lovley DR, Roden EE, Phillips EJP, Woodward JC. (1993). Enzymatic iron and uranium reduction by sulfate-reducing bacteria. *Marine Geol* **113**: 41-53.

Lovley DR, Widman PK, Woodward JC, Phillips EJP. (1993). Reduction of uranium by cytochrome c_3 of *Desulfovibrio vulgaris*. *Appl Environ Microbiol* **59**: 3572-3576.

Moura I, Bursakov S, Costa C, Moura JJG. (1997). Nitrate and nitrite utilization in sulfate-reducing bacteria. *Anaerobe* **3**: 279-290.

Mukhopadhyay A, He Z, Alm EJ, Arkin AP, Baidoo EE, Borglin SC *et al.* (2006). Salt stress in *Desulfovibrio vulgaris* Hildenborough: an integrated genomics approach. *J Bacteriol* **188**: 4068-4078.

Mukhopadhyay A, Redding AM, Joachimiak MP, Arkin AP, Borglin SE, Dehal PS *et al.* (2007). Cell-wide responses to low-oxygen exposure in *Desulfovibrio vulgatis* Hildenborough. *J Bacteriol* **189**: 5996-6010.

NABIR. (2003). Bioremediation of metals and radionuclides: what it is and how it works. In: Hazen TC, Benson SM, Metting FB, Faison B, Palmisano AC, McCullough J (Eds). NABIR primer, 2nd ed. Lawrence Berkeley National Laboratory: Berkeley, California, pp 1-78.

Nyman JL, Marsh TL, Ginder-Vogel MA, Gentile M, Fendorf S, Criddle C. (2006). Heterogeneous response to biostimulation for U(VI) reduction in replicated sediment microcosms. *Biodegradation* **17**: 303-316.

Payne RB, Gentry DA, Rapp-Giles BJ, Casalot L, Wall JD. (2002). Uranium reduction by *Desulfovibrio desulfuricans* strain G20 and a cytochrome c_3 mutant. *Appl Environ Microbiol* **68**: 3129-3132.

Pereira PM, He Q, Valente FMA, Xavier AV, Zhou J, Pereira IAC *et al.* (2008). Energy metabolism in *Desulfovibrio vulgaris* Hildenborough: insights from transcriptome analysis. *Antonie van Leeuwenhoek* **93**: 347-362.

Riley RG, Zachara JM. (1992). Chemical contaminants on DOE lands and selection of contaminant mixtures for subsurface science research DOE/ER-0547T. U.S. Department of Energy, Washington, D. C.

Rodionov DA, Dubchak I, Arkin AP, Alm E, Gelfand MS. (2004). Reconstruction of regulatory and metabolic pathways in metal-reducing δ-Proteobacteria. *Genome Biol* **5**: R90.

Stolyar S, He Q, Joachimiak MP, He ZL, Yang ZK, Borglin SE *et al.* (2007). Response of *Desulfovibrio vulgaris* to alkaline stress. *J Bacteriol* **189**: 8944-8952.

Valls M, de Lorenzo V. (2002). Exploiting the genetic and biochemical capacities of bacteria for the remediation of heavy metal pollution. *FEMS Microbiol Rev* **26**: 327-338.

van den Berg WAM, Hagen WR, van Dongen WMAM. (2000). The hybrid-cluster protein ("prismane protein") from *Escherichia coli*: characterization of the hybrid-cluster protein, redox properties of the [2Fe-2S] and [4Fe-2S–2O] clusters and identification of an associated NADH oxidoreductase containing FAD and [2Fe-2S]. *Eur J Biochem* **267**: 666-676.

Voordouw G, Grigoryan AA, Lambo A, Lin SP, Park HS, Jack TR *et al.* (2009). Sulfide remediation by pulsed injection of nitrate into a low temperature Canadian heavy oil reservoir. *Environ. Sci. Technol.* **43**: 9512-9518.

Wall JD, Krumholz LR. (2006). Uranium reduction. *Annu Rev Microbiol* **60**: 149-166.

Wall JD, Yen H-CB, Drury EC. (2007). Evaluation of stress response in sulphate-reducing bacteria through genome analysis. In: Barton LL, Hamilton WA (Eds). Sulphate-reducing bacteria: Environmental and engineered systems. Cambridge University Press: Cambridge, UK, pp 141-165.

Wang SC, Frey PA. (2007). *S*-adenosylmethionine as an oxidant: the radical SAM superfamily. *Trends Biochem Sci* **32**: 101-110.

Wei J, Sun J, Yu W, Jones A, Oeller P, Keller M *et al.* (2005). Global proteome discovery using an online three-dimensional LC-MS/MS. *J Proteome Res* **4**: 801-808.

Wolfe MT, Heo J, Garavelli JS, Ludden PW. (2002). Hydroxylamine reductase activity of the hybrid cluster protein from *Escherichia coli*. *J Bacteriol* **184**: 5898-5902.

Wolters DA, Washburn MP, Yates JRY, III. (2001). An automated multidimensional protein identification technology for shotgun proteomics. *Anal Chem* **73**: 5683-5690.

Titles and Legends to Figures:

Figure 1 Growth response of *Desulfovibrio vulgaris* to varying concentrations of **(A)** $NaNO_3$ or **(B)** NaCl.

Figure 2 Impact of glycine betaine on the growth of *D. vulgaris* exposed to 100 mM (**A**) and 200 mM (**B**) sodium nitrate. The inset in panel A shows the growth of *D. vulgaris* when 2 mM sodium nitrite was in place of sodium nitrate. *D. vulgaris* cultures were inoculated to a defined medium (Control, open circles), medium supplemented with sodium nitrate / nitrite only (open triangles), or medium supplemented with sodium nitrate / nitrite plus 2 mM glycine betaine as an osmoprotectant (closed triangles). Note different time scales on graphs. Results were typical of three experiments.

Figure 3 Gene expression overlap proportions between experimental time points of 8 different stress conditions for *D. vulgaris*, including nitrate, nitrite, NaCl, KCl, heat shock, low O_2 (1000 ppm), high O_2 (air), and alkaline (pH 10) stress. Shown are overlap proportions for genes in three categories: a) up-regulated; b) down-regulated; and c) both up- and down-regulated. The gene expression overlap proportion between two transcriptional profiles was computed as the number of genes above the threshold, i.e. Z-score and $\log_2$Ratio, common between a pair of transcriptional profiles normalized by the root of the product of the number of genes above threshold in each transcriptional profile. The nitrate, nitrite, and NaCl pairwise comparisons are in the top left corner of the heatmaps and are outlined in the black frame. Each square represents the gene expression overlap proportion of one pairwise comparison between two experiment time points. Time point increments for each stress condition progress left to right horizontally and top to bottom vertically from 30 min to 240 min post-stress. Solid black squares indicate cases where one or both of the experimental time points being compared had no genes with significant change in expression. The bright red squares along the diagonal correspond to the greater proportions of common genes between time points within the same experiment.

Figure 4 Conceptual model of responses to nitrate stress by *D. vulgaris* with linkages to both salt and nitrite stress in addition to shifts in energy metabolism. Colored symbols designate up-regulation. GBT: glycine/betaine ABC transporter; Hcp: hybrid cluster protein; PFL: pyruvate formate-lyase; PFLA: pyruvate formate-lyase activating enzyme; FDH: formate dehydrogenase; LDH: lactate dehydrogenase; AHP: alkyl hydroperoxide reductase; RBR: Rubrerythrin; RDL: Rubredoxin-like protein; SAM/Methyl cycle: *S*-adenosyl methionine cycle (details described in Figure S2).

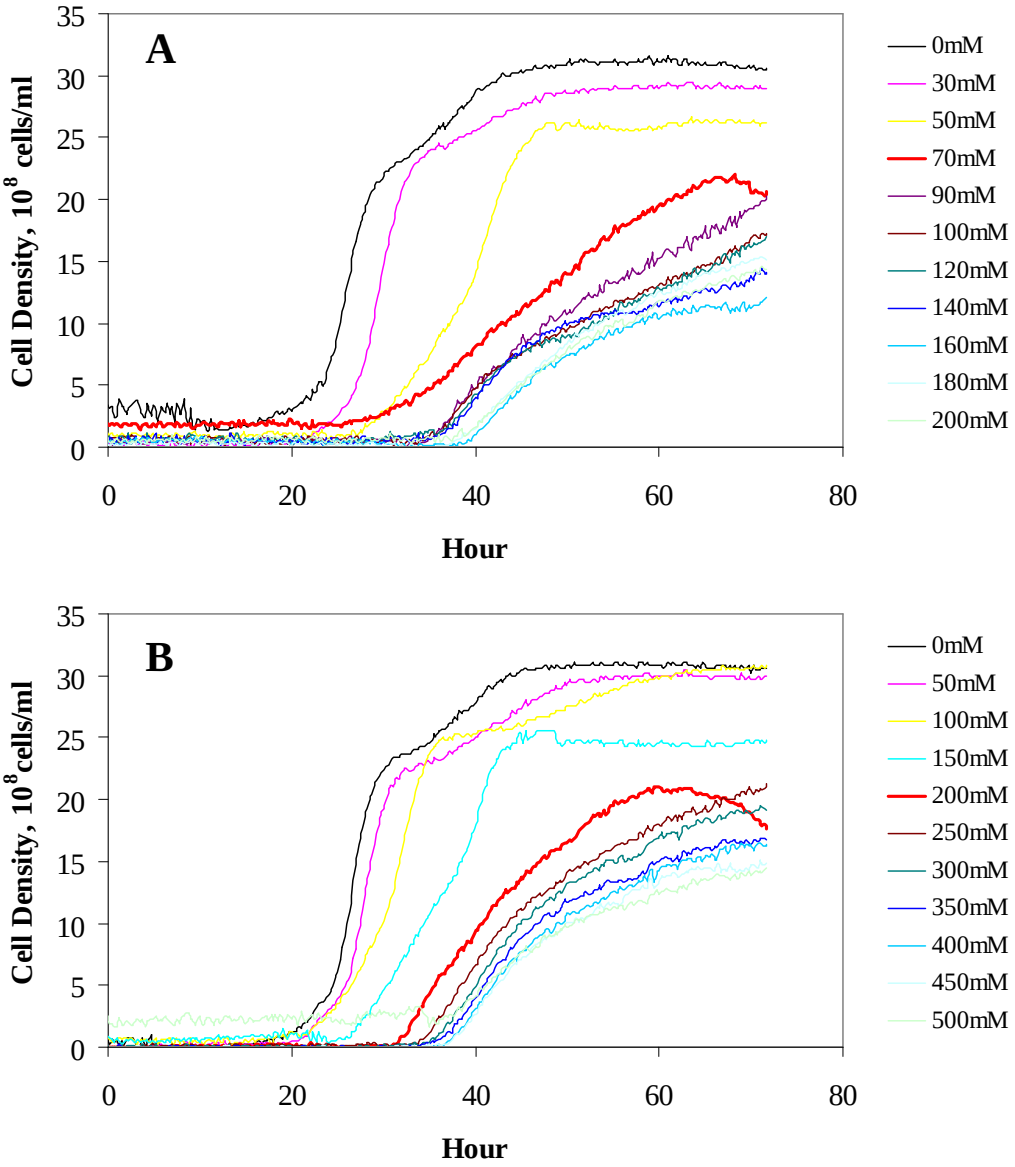
A
Cell Density, 10^8 cells/ml
Hour
0mM
30mM
50mM
70mM
90mM
100mM
120mM
140mM
160mM
180mM
200mM
B
Cell Density, 10^8cells/ml
Hour
0mM
50mM
100mM
150mM
200mM
250mM
300mM
350mM
400mM
450mM
500mM

Fig. 1

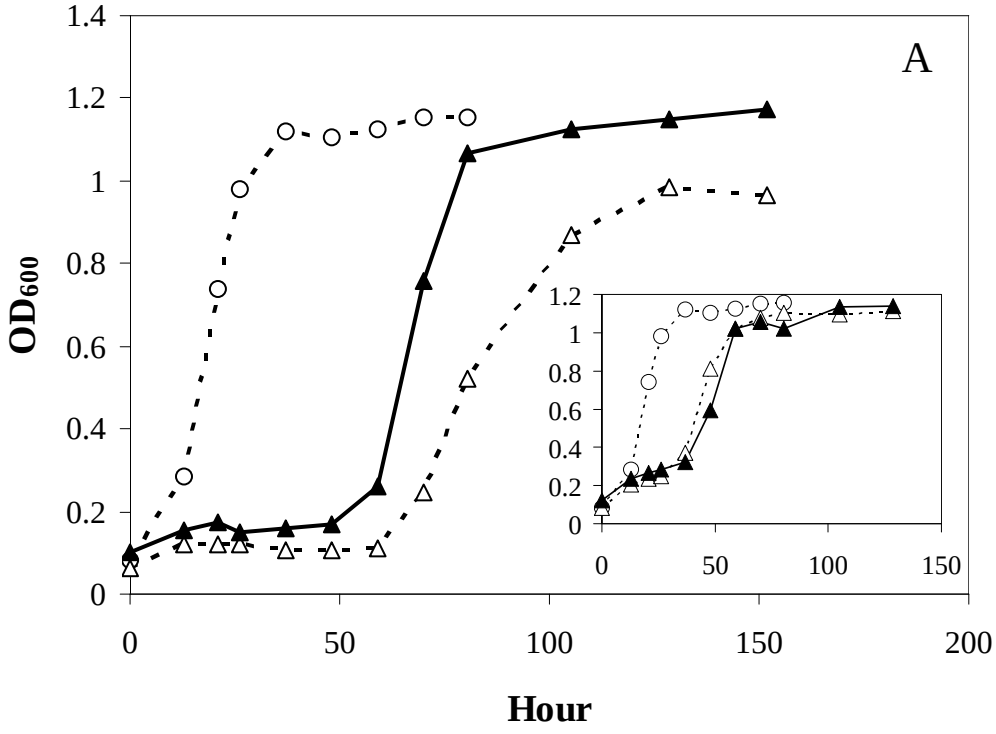
A
OD600
Hour
0
0.2
0.4
0.6
0.8
1
1.2
1.4
0
50
100
150
200

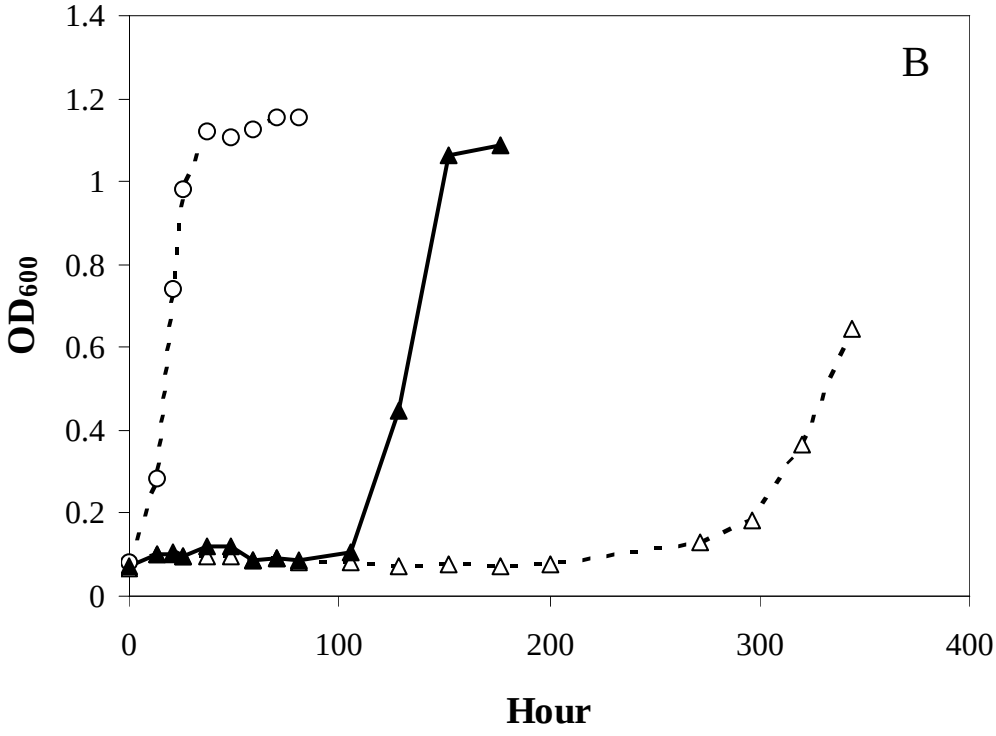
B
OD600
Hour
0
0.2
0.4
0.6
0.8
1
1.2
1.4
0
100
200
300
400

Fig. 2

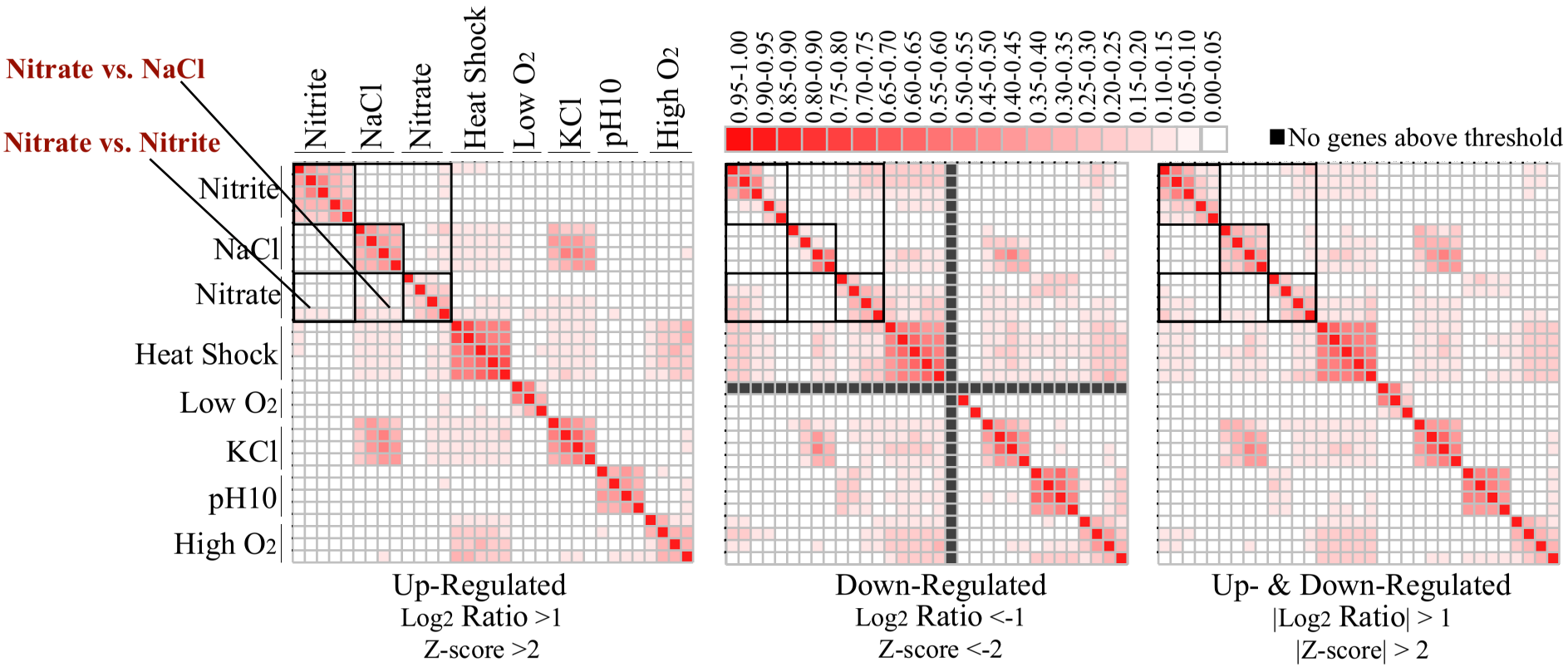
Nitrate vs. NaCl
Nitrate vs. Nitrite
Nitrite
NaCl
Nitrate
Heat Shock
Low O2
KCl
pH10
High O2
0.95-1.00
0.90-0.95
0.85-0.90
0.80-0.90
0.75-0.80
0.70-0.75
0.65-0.70
0.60-0.65
0.55-0.60
0.50-0.55
0.45-0.50
0.40-0.45
0.35-0.40
0.30-0.35
0.25-0.30
0.20-0.25
0.15-0.20
0.10-0.15
0.05-0.10
0.00-0.05
No genes above threshold
Up-Regulated
Log2 Ratio >1
Z-score >2
Down-Regulated
Log2 Ratio <-1
Z-score <-2
Up- & Down-Regulated
|Log2 Ratio| > 1
|Z-score| > 2

Fig. 3

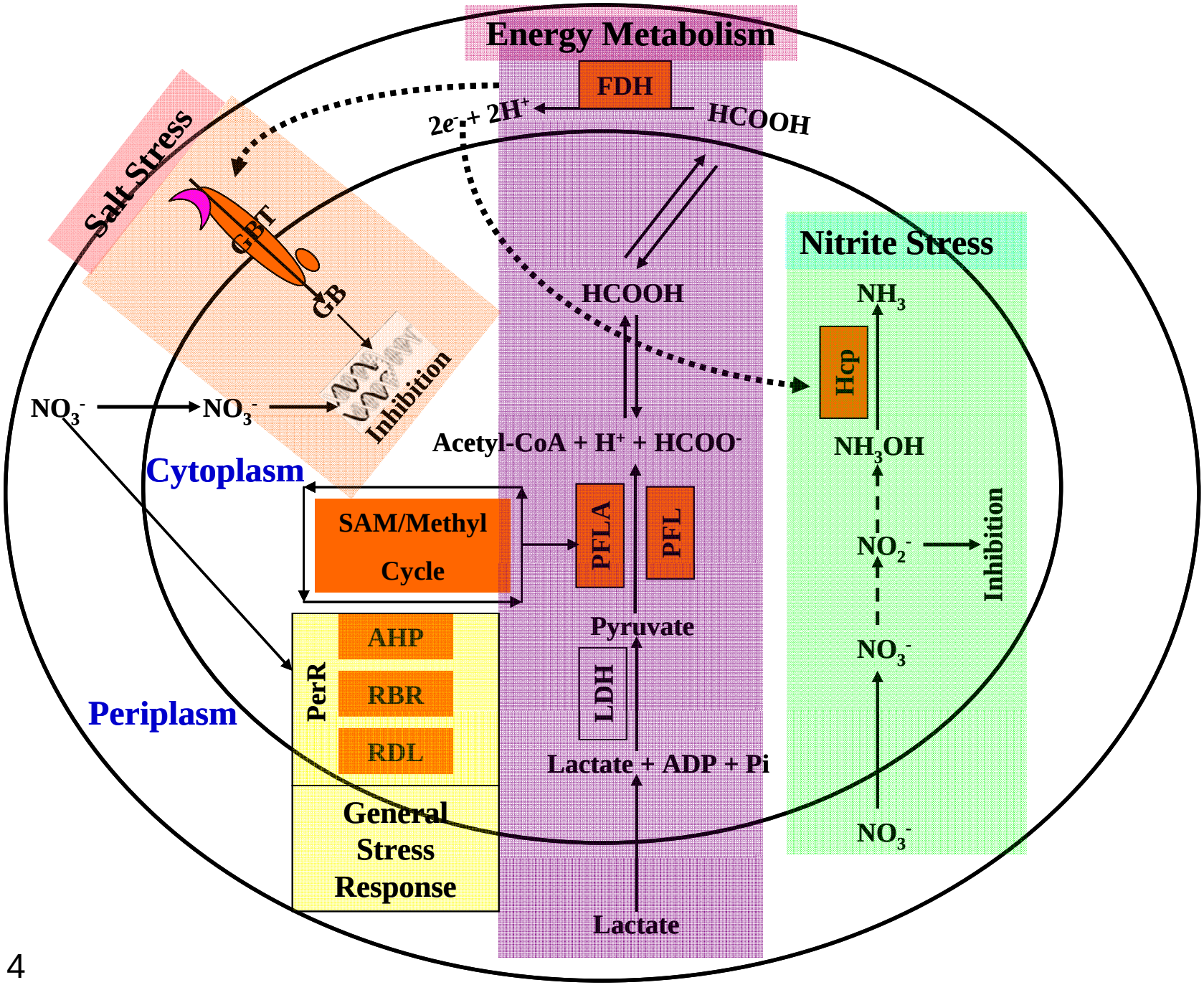
Energy Metabolism
FDH
HCOOH
2e- + 2H+
Salt Stress
GBT
GB
Inhibition
HCOOH
Nitrite Stress
NH3
Hcp
NH3OH
NO3-
NO3-
Inhibition
Acetyl-CoA + H+ + HCOO-
Cytoplasm
SAM/Methyl Cycle
PFLA
PFL
Pyruvate
LDH
Lactate + ADP + Pi
AHP
RBR
RDL
PerR
Periplasm
General Stress Response
NO2-
NO3-
Lactate

Fig. 4

Table 1. Comparison of gene expression of selected gene groups in response to $NaNO_3$, $NaNO_2$, and NaCl in *D. vulgaris*[a].

Gene ID	Log$_2$ Ratio of Transcriptional Response[b]			TIGR Annotation
	$NaNO_3$[c]	$NaNO_2$[c]	NaCl[c]	
Methyl metabolism				
DVU0606	**2.5**	**2.0**	-1.0	regulator/methyltransferase, UbiE/COQ5 family
DVU0607	**2.7**	**2.4**	1.1	adenosylhomocysteinase, AhcY
DVU0997	**2.9**	**2.2**	0.6	5,10-methylenetetrahydrofolate reductase, MetF
DVU2449	**1.7**	**2.1**	-1.3	*S*-adenosylmethionine synthetase, MetK
DVU3371	**2.7**	**3.8**	-1.4	5-methyltetrahydropteroyltriglutamate-homocysteine *S*-methyltransferase, MetE
Carbon metabolism				
DVU2822	**3.4**	0.9	**1.5**	TRAP dicarboxylate family transporter
DVU2823	**1.8**	0.4	1.9	TRAP dicarboxylate transporter family protein
DVU2824	**2.5**	0.5	0.9	formate acetyltransferase
DVU2825	**2.9**	0.6	0.7	pyruvate formate-lyase 1 activating enzyme
DVU0586	**2.5**	0.5	**-1.4**	Hypothetical protein
DVU0587	**1.5**	0.7	**-1.8**	formate dehydrogenase, alpha subunit, selenocysteine-containing
DVU0588	**1.6**	0.3	**-1.3**	formate dehydrogenase, beta subunit, putative
DVU1569	0.8	**1.1**	0.4	pyruvate ferredoxin oxidoreductase, alpha subunit PorA
DVU1570	-0.5	**1.3**	-1.2	pyruvate ferredoxin oxidoreductase, beta subunit PorB
Nitrogen metabolism				
DVU2543	**1.8**	**5.7**	**-1.2**	hybrid cluster protein
DVU2544	**1.9**	**6.2**	0.5	iron-sulfur cluster-binding protein
DVU0624	0.3	**4.4**	**-1.3**	NapC/NirT cytochrome *c* family protein
DVU0625	0.7	**4.1**	**-1.3**	cytochrome *c* nitrite reductase, catalytic subunit NrfA

[a]Gene expression profiles following $NaNO_3$ (105 mM), $NaNO_2$ (2.5 mM), and NaCl (250 mM) treatment in *D. vulgaris* were obtained from this study, He *et al.*, 2006, and Mukhopadhyay *et al.*, 2006, respectively.

[b]Expression ratios represent the highest levels of differential gene expression throughout the time course (240 min) of the stress exposure. Expression levels were obtained at the same time points from both the treatment and control cultures for the calculation of the expression changes resulting from the stressor. Positive Log$_2$ (Expression Ratio) values denote increases in expression level and negative values indicate decreases in expression level. Values with $Z > 2$ are shown in boldface type.

[c]The treatment cultures received addition of $NaNO_3$, $NaNO_2$, or NaCl, and the control cultures received none.

Table 2. Effect of nitrate exposure on the transcriptional responses of *Desulfovibrio vulgaris* genes in the predicted PerR regulon[a].

Gene ID	Description	Log_2 (Expression Ratio)[b]			
		30 min	**60 min**	**120min**	**240 min**
DVU0772	hypothetical protein	0.1	0.7	**2.0**	**2.4**
DVU2247	alkyl hydroperoxide reductase C, *ahpC*	0.2	0.5	0.7	**1.6**
DVU2318	Rubrerythrin, putative, *rbr2*	0.4	0.6	0.9	**2.2**
DVU3093	Rubredoxin-like protein, *rdl*	-0.2	0.0	0.8	**1.2**
DVU3094	Rubrerythrin, *rbr*	-0.2	-0.1	-0.3	0.7
DVU3095	Peroxide-responsive regulator PerR	-0.5	0.0	0.8	**1.4**

[a]Predicted PerR regulon from Rodionov *et al.*, 2004.

[b]Expression ratios represent the levels of gene expression at various time points following the addition of 105 mM nitrate into cultures compared to controls without nitrate addition. Expression levels were obtained at the same time points from both the treatment and control cultures for the calculation of the expression changes resulting from the stressor. Positive Log_2 (Expression Ratio) values denote increases in expression level and negative values indicate decreases in expression level. Values with $Z > 2$ are shown in boldface type.

Table 3. Comparison of transcript abundance with corresponding protein levels following nitrate exposure in *D. vulgaris*[a].

Gene ID	Description	Log_2(Expression Ratio)[b]	
		mRNA[c]	Protein[d]
DVU0470	Tryptophan synthase, beta subunit, *trpB-2*	+1.1[60]	+0.8
DVU0764	DNA-binding protein HU, *hup-2*	-1.1	-1.3
DVU0777	ATP synthase, F_1 alpha subunit, *atpA*	-1.1[120]	-0.4
DVU0873	Translation elongation factor Ts, *tst*	-1.4	+1.1
DVU1077	Inner membrane protein, 60 kDa, *yidC*	-1.3[120]	-1.0
DVU1089	Alanyl-tRNA synthetase, *alaS*	-1.3	+1.4
DVU1295	Sulfate adenylyltransferase, *sat*	+1.4	+0.4
DVU1300	Translation elongation factor G, *fusA-1*	-1.3	+0.5
DVU1303	Ribosomal protein L3, *rplC*	-1.7	-0.7
DVU1306	Ribosomal protein L2, *rplB*	-1.5	-1.0
DVU1308	Ribosomal protein L22, *rplV*	-1.7	-0.9
DVU1317	Ribosomal protein S8, *rpsH*	-1.3	-0.9
DVU1326	Ribosomal protein S13, *rpsM*	-1.2	-1.3
DVU1434	Hypothetical protein	-1.1	+2.0
DVU1443	Flagellar hook protein FlgE, *flgE*	-1.4[120]	-2.4
DVU1575	Ribose-phosphate pyrophosphokinase, *prsA*	-1.4	+1.5
DVU1636	Inorganic pyrophosphatase, manganese-dependent, *ppaC*	+1.2	+0.7
DVU1896	Ribosomal protein S20, *rpsT*	-2.1	-1.3
DVU2105	Hypothetical protein	-1.6[30]	-0.7
DVU2108	MTH1175-like domain family protein	+1.1[30]	+0.6
DVU2215	RNA-binding protein	-1.4[60]	+0.8
DVU2289	Hydrogenase, CooX subunit, putative, *b2488*	-1.1[120]	-2.0
DVU2297	Glycine/betaine/L-proline ABC transporter, periplasmic-binding protein	+1.6	+0.6
DVU2347	Acetylornithine aminotransferase, *argD*	+1.4	+0.8
DVU2364	Aminotransferase, classes I and II	-1.2[120]	-0.8
DVU2927	Ribosomal protein L7/L12, rplL	-1.5[120]	+0.9
DVU3228	Chemotaxis protein CheY, *cheY-3*	+1.0[120]	+1.3
DVU3371	5-methyltetrahydropteroyltriglutamate-homocysteine S-methyltransferase, *metE*	+2.7	+0.7

[a]Genes with significant changes at both the mRNA and protein levels (absolute value of Z > 2) subsequent to nitrate treatment were selected for comparison.
[b]Expression ratios represent the levels of expression following the addition of 105 mM nitrate into cultures compared to controls without nitrate addition. Expression levels were obtained at the same time points from both the treatment and control cultures for the calculation of the expression changes resulting from the stressor. Log_2(Expression Ratio) values greater than 0 denote increases in expression level and values less than 0 indicate decreases in expression level.

[c]Transcript abundance was determined from cDNA microarray analysis. Transcriptional expression ratios (log_2R) are shown for genes with Z > 2 (absolute value) at 240 min following nitrate treatment unless otherwise indicated. For genes with Z < 2 (absolute value) at 240 min, data are shown for a different time point (min; appears as an italic superscript).
[d]Protein abundance was determined from MS-MS proteomics analysis of protein extracts from cell samples subjected to 240-min of nitrate treatment. Protein abundance ratios (log_2R) are shown for genes with Z > 2 (absolute value) at 240 min following nitrate addition.